[1.]Ajay SHARMA, [2.]Sandeep Singh SANDHU, [3.]Vineet KUMAR

# ASSESSMENT OF MECHANICAL PROPERTIES OF THERMALLY AGED ELECTRON BEAM WELDED AISI 321 STAINLESS STEEL

[1,2.]Department of Mechanical Engineering, Quest Infosys Foundation Group of Institutions, Jhanjeri Mohali-140307 (Punjab), INDIA
[3.]Department of Mechanical Engineering, SUSIET, Tangori, Punjab, INDIA

**Abstract:** Electron beam welding produce very narrow and deep penetration therefore it has a great prospective in the welding of thick materials. AISI 321 is susceptible to inter-granular corrosion when it is subjected to thermal aging treatments, owing to the titanium depletion in weld zone. However, heat affected zone formed in electron beam welding extends to a narrow region across the weld pool. The present study electron beam welding of austenitic 321 stainless steel is done to examine the mechanical and metallurgical properties of the welds. Microhardness tests along and across the weld bead were carried out. Tensile and impact testing were performed for the analysis of mechanical properties. The microstructures of weld zone, fusion zone and base metals were also captured. It was found that skeletal ferrite and secondary carbides were found on the grain boundaries. The aging treatment of 700°C was given for 24 hours which resulted in change in morphology of the grains from skeletal to vermicular and promoted the formation Ti rich carbides. The maximum impact toughness conducted at subzero temperature i.e. -40°C was recorded as 129.3 J in as-welded samples and it got reduced to 119.5 J after aging treatment. The average ultimate tensile strength is 582 N/mm² and it got decreased to 481 N/mm² after aging treatment.
**Keywords:** Electron beam welding, thermal aging, mechanical properties, AISI 321 austenitic stainless steel

## 1. INTRODUCTION

Austenitic stainless steel AISI 321 has excellent corrosion resistance and oxidation properties. AISI 321SS grade steel applications is found in structural components, nuclear power plants and high-temperature components of boilers [1]. AISI 321 SS is derived from AISI 304 austenitic steel which is stabilized by the addition of Titanium element. Titanium diminishes the grain boundary sensitivity at high temperatures due to depletion of chromium carbides. This is why when it is heated within the range of 400-800°C, this grade is not sensitized to intergranular corrosion[2]. A.Prado et al.[3] concluded that addition of Ti in AISI 321 was not sufficient to prevent inter granular corrosion. They also concluded that annealing treatment with longer time for sensitization offer more resistance to inter granular attack. In most of the fusion welding methods, due to high heat input and dissolution of strengthening elements results in grain growth, reduction of mechanical properties and intergranular corrosion[4]. Welding of AISI 321 also very crucial as titanium forms oxides and weld zone get depleted of the stabalizing element. This make the weld zone more susceptible to interganular corrosion. Alali et al.[5] found equiaxed, columnar and dendritic ferrite in austenitic structure of EBW welded AISI 316. Further they also concluded that ultimate tensile of the specimen from the top was about 4% lower than the bottom specimen. M.B.Leban et al.[6] found Martensite, austenite polygarins with annealing twins and slip were present in the microstructure if crossion samples of AISI 321. Titanium nitrides inclusions were also found in the bottom of pits and in corrosion damage spots.

In engineering process like fabrication, maintenance and repair welding plays very important role. Large amount of thermal stress are produced during welding due to the localised heat near the weld region[7].

ANNALS of Faculty Engineering Hunedoara – International Journal of Engineering
ISSN 1584 - 2665 (printed version); ISSN 2601 - 2332 (online); ISSN-L 1584 - 2665
Universitatea Politehnica Timişoara

Subsequent cooling after welding result in distortion, residual stresses and large heat effected zone[8]. Electron beam welding (EBW) is becoming more popular in the manufacturing of engineering parts as it produce joints with less distortion and heat effected zone is also very less. An exceptional feature of EBW is its ability to make extremely narrow, deep welds even for the thick plates[9]. Ting Wang et al. [10] showed that joint produced using EBW had the highest tensile strength of which was 83% more than that of base metal. Wu Bing et al. [11] made the electron beam joint of casting TC4 (ZTC4) alloy and found acicular martensites were present in the weld region. They also concluded that the tensile strength of weld joints is higher than that of the base metal.

A lot of work has been reported on the welding of AISI 321using different welding techniques. These welds were evaluated for microstructure properties, impact toughness and tensile behaviour in the as-welded condition. Thermal cycle's induced during welding processes generates greater heat affected zone, residual stresses and cold cracking susceptibility in the weld metal. To get rid of these problems post weld thermal aging (PWTA) after welding is employed. No work has been reported on PWTG of the EBW welded AISI 321 SS. The present work was aimed to investigating 18 mm thick electron beam welded butt joints of AISI 321 stainless steel in the as-welded and thermally aged at 750°C for 24 hours. Butt welds were examined for impact toughness and tensile behaviour and its affect on the microhardness and microstructure properties.

## EXPERIMENTAL PROCEDURE

Two AISI 321 plates of 18 mm thickness and size 200mm x 75mm were welded using EBW process. The chemical composition of the base material is shown in table 1. The welding was done without filler metal. A backing plate is attached to the plates so that full penetration can take place.

Table 1: Composition ranges for 321 grade stainless steel

| Grade | | C | Mn | Si | P | S | Cr | Ni | N | Other | Fe |
|---|---|---|---|---|---|---|---|---|---|---|---|
| 321 | min. | - | 2.00 | 0.75 | 0.045 | 0.030 | 17.0 | 9.0 | 0.10 | 0.70 | Bal |
| | max | 0.08 | | | | | 19.0 | 12.0 | | | |

Table 2: Welding Parameters

| Accelerating Voltage (HV) kV | Beam Current (SQ) mA | Focus Coil Current (SL) mA | Welding Speed (SP) mm/min | Oscillation Pattern | Heat Input kJ/min |
|---|---|---|---|---|---|
| 150 | 90 | 2210 | 600 | Line | 1.28 |

The welding parameters are shown in table 2. After welding the welding joints were inspected using die penetration test and ultrasonic nondestructive testing techniques to ensure the sound welds.

Specimens for Transverse tensile test specimens were prepared in accordance of ASTM: E8/E8M-13a[12]. Six samples were cut from the weld plate. PWTG treatment of 750°C for 24 hours was given to three samples. Then after as welded samples and thermally aged samples were tested on universal testing machine "*Tinius H50KS*". Ultimate tensile strength (UTS), yield strength (YS) fracture location and percentage elongation were recorded. To evaluate the toughness of the welded joint Charpy V-notch impact strength of the all welds is evaluated. The 12 samples of Charpy V-notch were extracted according to the ASTM: E23-12c[13]. Six samples were given PWTA treatment of 750°C for 24 hours. Impact test was conducted at the sub-zero temperature using charpy impact testing machine of 3 ton capacity. Four samples of size 10 x 10x 18 mm were cut and two samples were given PWTA treatment. Then microhardness was performed on two samples one as welded and one thermally aged sample according to ASTM: E-384-11e1[14] using Vickers micro hardness testing machine. The remaining two samples were prepared as metallographic specimens. First grinding was done on bench grinder using grinding wheel of grade 80 to achieve a flat surface. They were polished using emery papers from grades 100 to 2000 on the polishing machine. After that etching of each specimen was done using Marbel's reagent to reveal the microstructure. The microstructure images were also carried out using optical microscope at different magnifications.

## 2.RESULTS AND DISCUSSIONS

### —Metallography and image analysis

The Macrostructure view of the EBW weld joint of AISI 321 is shown in Figure 1. The penetration of the weld bead is complete through the material thickness. Dagger shaped weld bead is seen in

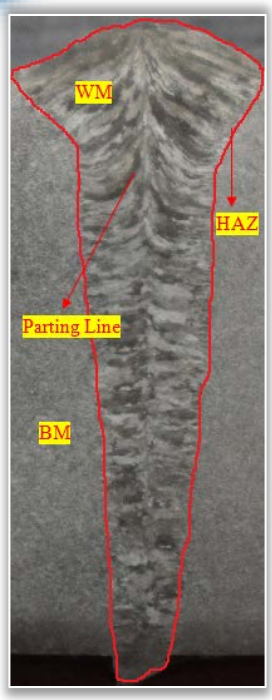


Figure 1: Macrostructure of EBW welds showing base metal (BM), weld metal (WM) and heat affected zone (HAZ)

the macrostructure having three regions base metal (BM), Heat affected zone (HAZ) and Weld metal (WM). Through weld can be seen in the macrostructure.

The microstructure of the Base metal is shown in Figure 2. The base metal shows step microstructure containing austenite grains. The coarsening of austenite grains can be easily seen identified in the base metal and TiN particles are also seen in the microstructure (indicated by arrows). Same structure was observed by M.Tavares et al.[15]. Figure 3 shows the microstructure of the fusion zone and weld zone in as-welded and after PWTA treatment.

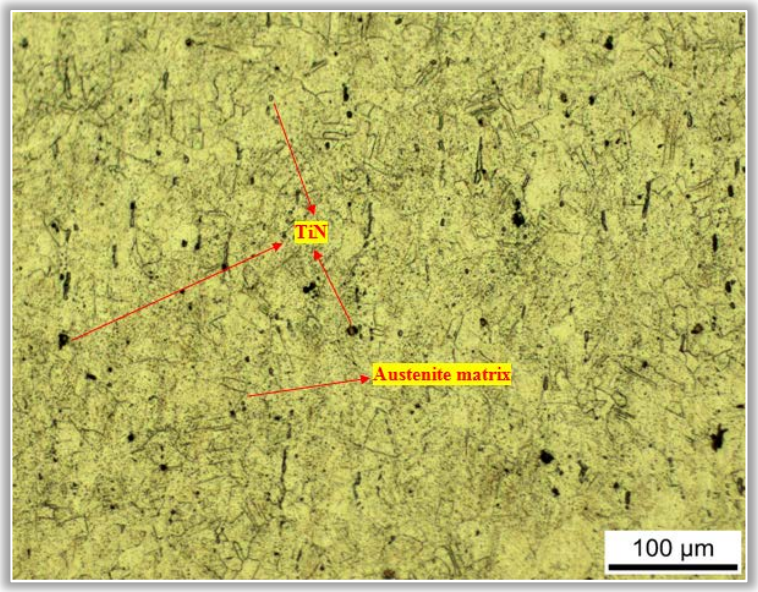


Figure 2: Microstructure showing base metal (BM) AISI 321

Weld metal consist of austenitic matrix with skeletal morphology of δ-ferrite on the side of the grain boundaries in both as-welded and thermally aged samples. This may be resulted due to the high cooling rate in the EBW process[16].

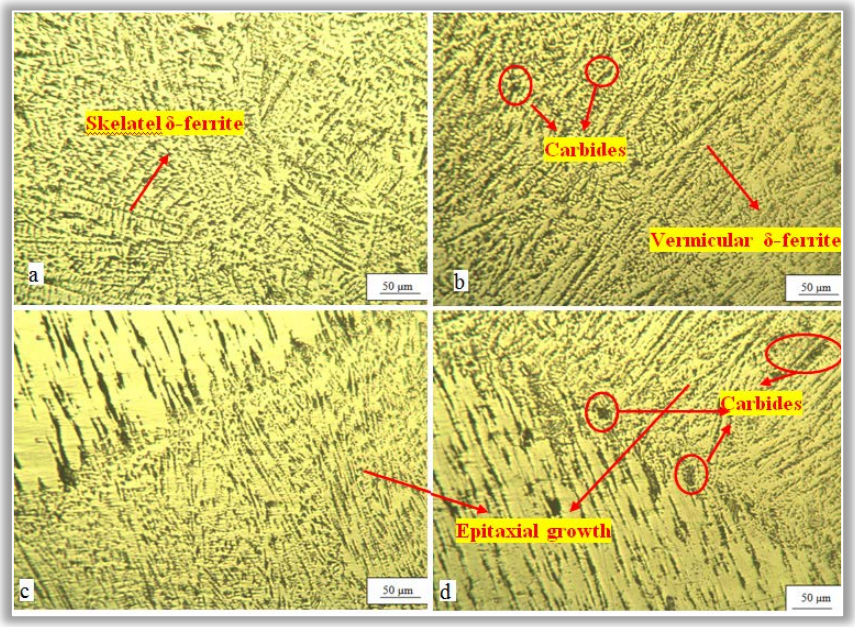


Figure 3: Microstructure of weld metal and fusion zone (a), (b) microstructure of weld zone shows precipitation in as-welded and thermally aged condition respectively. (c), (d) microstructure of fusion zone shows carbide precipitation in as-welded and thermally aged condition respectively

Figure 3(a) shows the microstructure of the weld zone in as welded condition, which shows the presence of skeletal δ-ferrite structures. Figure 3(b) shows the microstructure of the weld zone after thermal aging treatment. Vermicular structures of δ-ferrite dendrites can be seen.[17] The

precipitation of carbides in the austenitic matrix can be identified in the microstructure. Less δ ferrites were detected in the weld metal after aging 24 h at 750°C. K. Guan et al.[18] reported that δ ferrite, distributing mainly at the grain boundaries is transformed to α- phase during high-temperature aging. It may be due to superior cooling rates of the weld bead. Figure 3c shows the fusion zone of the as-welded sample. The epitaxial growth of the austenite is seen near the fusion line in both as welded and thermally aged sample. The figure 3d shows the micro structure of thermally aged sample.

### — Microhardness analysis

The microhardness variations along the weld is shown in figure 4. The microhardness in the as-welded conditions is more than aging treatment has decreased the microhardness value by approximately 8% all through the weld bead. The precipitation of the δ ferrite along the grain boundaries may be the reason for this decrease. Mourad et al.[19] has also observed that the ferrite content effect the hardness of the weld metal. The hardness value is also increased from top to bottom of the weld. Rapid cooling may be the reason for this increase in the hardness. Figure 5 shows the average microhardness of the BM, WM and HAZ for both as welded and thermally aged samples. The average microhardness BM HAZ and WM is 187 HV, 197.1 HV and 206.7 HV respectively for as-welded condition. The microhardness of the weld zone is higher than the base metal. This could be because precipitation of the ferrite phase and finer microstructure due to the faster cooling rate in EBW. Overall the results showed that the aging reduce hardness slightly even though carbides are present in the welds. The average microhardness BM HAZ and WM is 178.1 HV, 196.6 HV and 202.8 HV respectively for thermally aged condition.

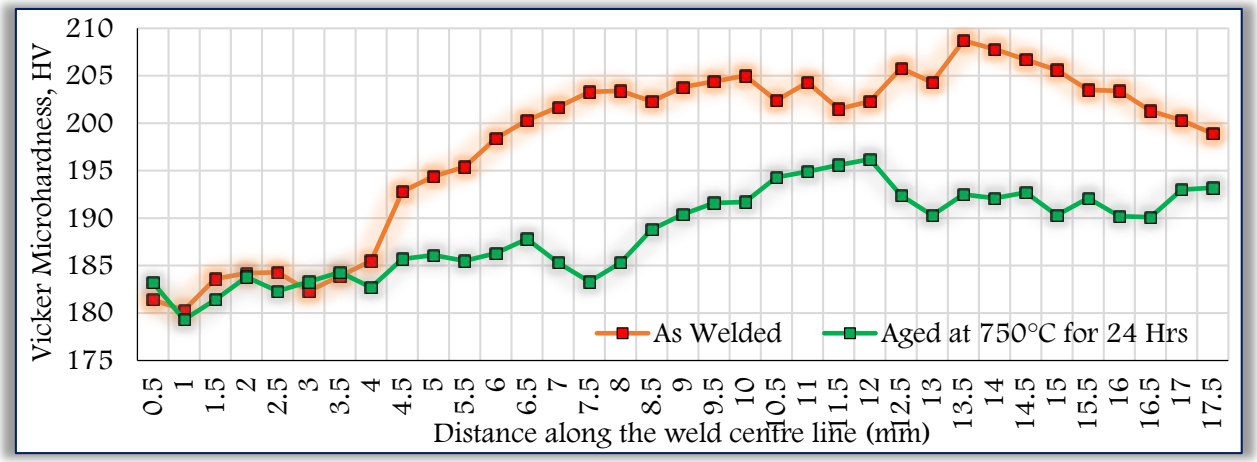


Figure 4. Microhardness variations along the weld

## 3. MECHANICAL TESTING

### — Impact Toughness

All the weldments undergo notch deformation and ductile fracture was seen. The maximum impact energy of 129.3J was absorbed by the sample in as welded condition. The aging treatment reduced the impact toughness to 119.5 as compare to as welded specimens. This may be due to carbide prescription in the weld zone. K. Guan et al.[20] also concluded that increased amount of precipitate decreases the impact energy as the aging time increases.

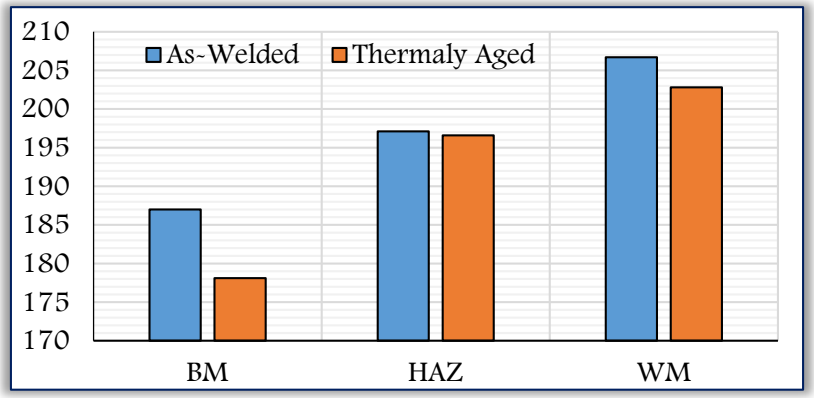


Figure 5. The average microhardness of the BM, WM and HAZ for both as welded and thermally aged

— Tensile Studies

Tensile studies were carried out at room temperature. The figure 6 shows the tensile test results. All samples failed from the weld metal, which shows that weld metal was weaker then the base metal. On the contrary yilbas et al.[9] reported failure from the weld metal. The yield strength and ultimate strength slightly reduced after the thermal aging. But the percentage elongation has increased after thermal aging treatment. The yield strength is almost closer to the base metal.

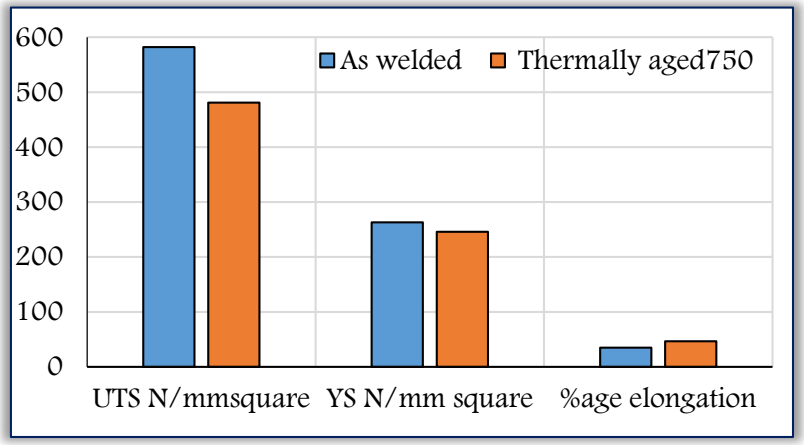


Figure 6: Tensile test results for EBW as –welded and thermally aged samples

## 4. CONCLUSIONS

The present work reported the mechanical properties, metallurgical characteristic in as welded state and after post welds thermal aging (750° C for 24 hours), 18 mm thick austenitic stainless steel AISI 321 was joined using EBW. The following conclusions can be made from the study:

— Finer grains are formed in the weld metal as compared to base metal because of the rapid cooling of the weld metal.

— Skeletal and vermicular δ-ferrite on the side of the grain boundaries in weld meal in both as-welded and thermally aged samples. The formation of carbides is seen after the thermal aging treatment which also results in reduction of volume of δ-ferrite. Epitaxial growth is seen in fusion zone.

— The microhardness is reduced along the weld bead. It has the highest value in the weld metal because of formation of finer grain in the weld metal.

— Impact strength and tensile strength is reduced after the thermal aging treatment. All the failures in the tensile test occur in the weld metal which shows the weld metal has lees ultimate strength then the base metal.

## References

[1] S. Mohan Kumar and N. Siva Shanmugam, "Studies on the weldability, mechanical properties and microstructural characterization of activated flux TIG welding of AISI 321 austenitic stainless steel," Mater. Res. Express, vol. 5, no. 10, 2018.

[2] M. S. Ghazani and B. Eghbali, "Characterization of the hot deformation microstructure of AISI 321 austenitic stainless steel," Mater. Sci. Eng. A, vol. 730, pp. 380–390, Jul. 2018.

[3] A. Pardo, M. C. Merino, A. E. Coy, F. Viejo, M. Carboneras, and R. Arrabal, "Influence of Ti , C and N concentration on the intergranular corrosion behaviour of AISI 316Ti and 321 stainless steels," vol. 55, pp. 2239–2251, 2007.

[4] M. Nabahat, K. Ahmadpour, and T. Saeid, "Effect of ultrasonic vibrations in TIG welded AISI 321 stainless steel: Microstructure and mechanical properties," Mater. Res. Express, vol. 5, no. 9, 2018.

[5] M. Alali, I. Todd, and B. P. Wynne, "Through-thickness microstructure and mechanical properties of electron beam welded 20 mm thick AISI 316L austenitic stainless steel," Mater. Des., 2017.

[6] M. B. Leban and R. Tisu, "The effect of TiN inclusions and deformation-induced martensite on the corrosion properties of AISI 321 stainless steel," Eng. Fail. Anal., 2013.

[7] S. Nakhodchi, A. Shokuhfar, S. A. Iraj, and B. G. Thomas, "Evolution of temperature distribution and microstructure in multipass welded AISI 321 stainless steel plates with different thicknesses," J. Press. Vessel Technol. Trans. ASME, vol. 137, no. 6, 2015.

[8] D. Karthik and S. Swaroop, "Effect of laser peening on electrochemical properties of titanium stabilized 321 steel," Mater. Chem. Phys., 2017.

[9] B. S. S. Yilbas, M. Sami, J. Nickel, a. Coban, and S. a. M. A. M. Said, "Introduction into the electron beam welding of austenitic 321-type stainless steel," J. Mater. Process. Technol., vol. 82, no. 1–3, pp. 13–20,

1998.
[10] Y. Zhang, T. Wang, S. Jiang, B. Zhang, Y. Wang, and J. Feng, "Microstructure evolution and embrittlement of electron beam welded TZM alloy joint," Mater. Sci. Eng. A, 2017.
[11] W. Bing, L. Jinwei, and T. Zhenyun, "Study on the Electron Beam Welding Process of ZTC4 Ti- tanium Alloy," 2014.
[12] ASTM E8, "ASTM E8/E8M standard test methods for tension testing of metallic materials 1," Annu. B. ASTM Stand. 4, no. C, pp. 1–27, 2010.
[13] ASTM E 23-12c, "Standard Test Methods for Notched Bar Impact Testing of Metallic Materials," Standards, vol. i, pp. 1–25, 2013.
[14] American Society of Testing and Materials (ASTM), "Standard Test Method for Microindentation Hardness of Materials - ASTM E384," ASTM Stand., vol. 14, pp. 1–24, 2002.
[15] A. Y. Kina, V. M. Souza, S. S. M. Tavares, J. A. Souza, and H. F. G. de Abreu, "Influence of heat treatments on the intergranular corrosion resistance of the AISI 347 cast and weld metal for high temperature services," J. Mater. Process. Technol., 2008.
[16] J. Swaminathan, R. Singh, M. K. Gunjan, and B. Mahato, "Sensitization induced stress corrosion failure of AISI 347 stainless steel fractionator furnace tubes," Eng. Fail. Anal., 2011.
[17] K. D. Ramkumar, A. Chandrasekhar, A. K. Singh, S. Ahuja, A. Agarwal, N. Arivazhagan, and A. M. Rebel, "Comparative studies on the weldability, microstructure and tensile properties of autogeneous TIG welded AISI 430 ferritic stainless steel with and without flux," J. Manuf. Process., 2015.
[18] K. S. Guan, X. D. Xu, Y. Y. Zhang, and Z. W. Wang, "Cracks and precipitate phases in 321 stainless steel weld of flue gas pipe," Eng. Fail. Anal., 2005.
[19] A. H. I. Mourad, A. Khourshid, and T. Sharef, "Gas tungsten arc and laser beam welding processes effects on duplex stainless steel 2205 properties," Mater. Sci. Eng. A, vol. 549, pp. 105–113, 2012.
[20] K. Guan, X. Xu, H. Xu, and Z. Wang, "Effect of aging at 700 °c on precipitation and toughness of AISI 321 and AISI 347 austenitic stainless steel welds," Nucl. Eng. Des., 2005.

ANNALS of Faculty Engineering Hunedoara – International Journal of Engineering
ISSN 1584 - 2665 (printed version); ISSN 2601 - 2332 (online); ISSN-L 1584 - 2665

http://annals.fih.upt.ro